

Session I - 1.3

MAGNETIC FIELD: MEASUREMENTS AND MODELS

The inference of the magnetic field vector in prominences

Bruce W. Lites

High Altitude Observatory, National Center for Atmospheric Research,
P.O. Box 3000, Boulder, CO 80307-3000, USA
email: lites@ucar.edu

Abstract. Prominences owe their existence to the presence of magnetic fields in the solar corona. The magnetic field determines their geometry and is crucial to their stability, energetics, and dynamics. This review summarizes techniques for measurement of the magnetic field vector in prominences. New techniques for inversions of full Stokes spectro-polarimetry, incorporating both the Zeeman and Hanle mechanisms for generation and modification of polarization, are now at the forefront. Also reviewed are measurements of the magnetic fields in the photosphere below prominences, and how they may be used to infer the field geometry in and surrounding the prominence itself.

Keywords. magnetic fields, polarization, scattering, data analysis, polarimetric, Sun: prominences, Sun: filaments

1. Introduction

The major, but still incompletely understood aspects of the nature of prominences – their origin, topology, stability, and relationship to dynamic events in the corona – are intimately connected to the magnetic field. The ultimate observational objective would be to obtain precision measures of the magnetic field *vector* in the three-dimensional volume from the photosphere below the prominence, within the prominence itself, and to the larger coronal volume above and surrounding it. Were we able to attain this goal, our understanding of this phenomenon would be far more complete. Alas, this ideal observational picture of the field is beyond our current capability. However, within the last few years significant progress has been realized toward this ultimate goal – remote sensing of the magnetic field vector in and surrounding prominences – through new observations and development of advanced data analysis methods. Furthermore, the prospect of a dramatic advance of observational capability for precision polarimetry, using ground- and space-based facilities either under development or in the planning stages, promises to bring us much closer to this ultimate goal.

It is possible to infer some properties of the magnetic field vector using indirect methods, examples of which are intensity tracers for field alignment (see Lin *et al.* 2005), line profile diagnostics at various wavelengths including the ultraviolet (Schmieder *et al.* 2007), and dynamical response to external perturbations (i.e. the “winking filaments” of Hyder 1966). Indirect techniques provide important information regarding the magnetic field; information that is often needed to properly interpret direct methods (e.g. in resolution of the 180° azimuth ambiguity), but due to limitations of space and scope, this review concentrates on “direct” inference of the magnetic field vector, primarily through polarimetric means.

Despite the importance of the magnetic field, over the years there have been relatively few attempts to measure it in prominences, likely owing both to the difficulty of the measurements and the interpretation of the data. One source of the observational challenge is

the paucity of suitable spectral diagnostics. There are only a handful of spectral features in the solar spectrum that present good polarimetric diagnostics of the magnetic field at (chromospheric) temperatures and densities typical of the conditions in prominences. Precision polarimetry is needed to make reliable field measurements, so one requirement of a spectral diagnostic is that there be significant optical depth in the body of the prominence (or filament if seen against the disk) in order to detect a sufficient photon flux. In practice this requirement has limited the diagnostics to spectra of the abundant elements H and He. The atomic processes governing the generation of polarized radiation in the spectra of H and He, especially at the lower chromospheric densities typical of prominences where scattering dominates the radiative transport, only recently have been fully understood. With the advent of new observational facilities and diagnostic tools grounded upon rather complete treatments of the atomic physics, a new era in measurement of the magnetic field in prominences is now upon us.

Section 2 of this review presents a brief summary of the history of inference of magnetic fields in prominences and filaments. Section 3 outlines results of measurement of the photospheric fields below prominences. Section 4 is a discussion of the possibilities for future measurement of prominence magnetic fields.

2. A Perspective on Measurement of Prominence Magnetic Fields

To date there have been few reviews of magnetic field measurements in prominences. The reader is referred to reviews by Paletou & Aulanier (2003), López Ariste & Aulanier (2007), Paletou (2008), and Mackay *et al.* (2010). Table 1 presents a selection of milestones for prominence field measurements to date. Early attempts at measurement of the prominence field used standard longitudinal magnetometry: considering the circular polarization signal only. These studies assumed that the polarization signal results from the Zeeman effect in $H\alpha$, $H\beta$, and/or He I D_3 (Zirin & Severny 1961, Rust 1967, Harvey 1969, Tandberg-Hannsen 1970). These observations did not resolve the Stokes V line spectrally, so that the authors could not know that the profiles often had anomalous shapes (López Ariste *et al.* 2005); that is, rather than being antisymmetric about line center, the Stokes V profiles can exhibit a symmetric shape arising as a result of a scattering process. As pointed out much later by Brown, López Ariste, & Casini (2003), in spite of the interpretative mechanism being in error these early magnetographic inferences yielded plausible field strengths because both the Zeeman effect and scattering in the presence of an anisotropic radiation field induce approximately the same Stokes V polarization levels.

2.1. Early Application of the Hanle Effect to Prominence Measurements

Hyder (1965) reported measurements of linear polarization in the $H\alpha$ line for 16 prominences. In that work he was able to measure the orientation of the linear polarization, but not its magnitude, and found that the orientation was not strictly tangential to the solar limb as would be expected from scattering in the non-magnetic case. He then interpreted the observed orientation of the linear polarization as arising from scattering in the presence of a magnetic field (the Hanle effect). In the Hanle effect, both the degree of polarization and its orientation depend on the strength of the field. Without precision measurements of the degree of polarization, accompanied by a sophisticated analysis, no definitive conclusions could be drawn regarding the magnetic field strength and its orientation.

Much later, Leroy and co-workers (Leroy 1977; Leroy 1978; Bommier, Sahal-Brechot, & Leroy 1981; Leroy, Bommier, & Sahal-Brechot 1983, 1984; Bommier *et al.* 1994; Bommier

Table 1. Milestones in Measurement of Prominence Magnetic Fields.

Reference	Method	Field Attributes
Zirin 1961	Zeeman magnetometry $H\alpha$	[<i>few</i> \times 100 G, < 2 G] for [active, quiet]
Hyder 1964, 1965	scattering rotation of linear pol. (Hanle effect) $H\alpha$	<i>few</i> \times 10 G
Rust 1967	Zeeman magnetometry $H\alpha$	5-60 G
Harvey 1969	Zeeman magnetometry $H\alpha$, He I D_3	0-15 G
Tandberg-Hanssen 1970	$H\alpha$, He I D_3 , others, Zeeman magnetometry	<i>few</i> G, aligned to prom. axis
Leroy 1977b, 1978, 1983 Leroy <i>et al.</i> 1984	Hanle effect I, Q, U He I D_3 Hanle magnetometry He I D_3 ($+H\alpha$)	0-10 G, horiz. field small angle to prom. axis
House & Smart 1982 Landi degl'Innocenti 1982 Athay <i>et al.</i> 1983	Hanle spectro-polarimetry He I D_3 (allows meas. of all 3 field comp.) inversion code for complete I, Q, U, V	horiz. field tendency for inverse config.?
Querfeld <i>et al.</i> 1985	spectro-polarimetry He I D_3 Gaussian fits to profiles	Stokes V is necessary
Bommier <i>et al.</i> 1994, 1998	Hanle magnetometry He I D_3 ($+H\alpha$)	< 10 G, horizontal, inverse config.
H. Lin <i>et al.</i> 1998	spectro-polarimetry He I 10830 Å Stokes U analysis only	filament on disk
López Ariste & Casini 2002, 2003, Casini <i>et al.</i> 2003 Brown <i>et al.</i> 2003 Schmieder <i>et al.</i> 2013	spectro-polarimetry He I D_3 quantum interferences in incomplete Paschen-Back regime, PCA inversion	spectrally resolved I, Q, U, V $ \mathbf{B} \sim 10$ -20 G but some $ \mathbf{B} > 50$ G
Trujillo Bueno <i>et al.</i> 2002	spectro-polarimetry He I 10830 Å lower level atomic polarization	<i>a few</i> G, highly inclined
López Ariste <i>et al.</i> 2005	I, Q, U, V spectro-polarimetry $H\alpha$	scattering polariz. Stokes V non-Zeeman, electric fields?
Merenda <i>et al.</i> 2006	spectro-polarimetry He I 10830 Å complete treatment Hanle + Zeeman	vertical fields in polar crown prominence
Kuckein <i>et al.</i> 2012	spectro-polarimetry He I, Si I 1083nm Zeeman effect only	active region filament 3-D structure \rightarrow flux rope
Orozco Suárez <i>et al.</i> 2013	spectro-polarimetry He I 10830 Å complete Hanle-Zeeman analysis	$ \mathbf{B} $ 5-30 G, incl. 65 – 75°

& Leroy 1998) carried out analyses of quantitative measures of the linear polarization observed primarily in the He I D_3 line in quiescent prominences (Leroy 1977). Their analysis is based on computations of the modification of scattering polarization due to the Hanle effect (Sahal-Brechot, Bommier, & Leroy 1977, Bommier & Sahal-Brechot 1978, Bommier 1980). The observations did not resolve the spectral lines, so that the basic data consisted of two pieces of information: the degree of polarization and its angular orientation in the plane of the sky. Three independent measures are needed to fully specify the magnetic field vector, the ambiguity associated with the polarization orientation notwithstanding. Adopting the assumption that the prominence field is largely horizontal (Leroy 1978) allowed Sahal-Brechot, Bommier, & Leroy (1977), Leroy (1977) and Leroy (1978) to infer the field strength and the angle of the field in the horizontal plane. The analysis proceeds from a forward synthesis of the line polarization, resulting in a *Hanle effect polarization diagram* (for example, Fig. 5 of Sahal-Brechot, Bommier, & Leroy 1977) in which separate sets of contours of constant field strength and constant inclination to the line-of-sight are plotted against the angle of linear polarization in the plane of the sky (on the abscissa) and polarization degree (on the ordinate). Each of the observed data may then directly indicate the field strength and inclination.

Using simulations of lines, Bommier, Sahal-Brechot, & Leroy (1981) reported that the most effective method to augment the Hanle effect observations to allow a complete de-

termination of the magnetic field vector was to obtain simultaneous measurements in two or more different lines having differing sensitivities to the Hanle effect. Following this reasoning, Leroy, Bommier, & Sahal-Brechot (1984) then interpreted measurements of many prominences, a significant fraction of which included simultaneous measurements in He I D_3 plus either $H\alpha$ or $H\beta$. Although the hydrogen line data were not included explicitly in their analysis, they independently confirmed that fields are close to horizontal in quiescent prominences. More detailed analysis of simultaneous measurements in He I D_3 and $H\beta$ (Bommier, Sahal-Brechot, & Leroy 1986), then in He I D_3 plus $H\alpha$ (Bommier *et al.* 1994), indicate that most quiescent prominences have fields that are nearly horizontal, and have “inverse configuration” with respect to the photospheric field below (that is, the sense of the field component perpendicular to the prominence axis is negative toward positive polarity, as opposed to the potential field case).

In the foregoing two-line analyses the authors confronted the complications of generation of scattering polarization in the hydrogen Balmer lines. In addition to treatment of the scattering process in the optically-thick non-LTE transfer of the $H\alpha$ line, it was necessary to treat the detailed quantum electrodynamics formulation of scattering polarization and collisional interaction via the density matrix formulation. The formulation of the problem and its forward solution for the prominence case are outlined in Landi Degl’Innocenti, Bommier, & Sahal-Brechot (1987). They present Hanle effect polarization diagrams for $H\alpha$. The unavoidable ambiguity of the magnetic field azimuth arising from any polarization diagnostic takes a different form when the line becomes optically thick. For the Zeeman effect and optically-thin Hanle effect diagnostics the ambiguity of the inferred field vector is symmetric with respect to the line-of-sight, but in the optically-thick scattering case the two-fold ambiguous field vectors no longer display that symmetry. It is noted that this broken symmetry provides an observational basis for resolution of this fundamental ambiguity (Bommier *et al.* 1994).

2.2. *The Modern Era of Magnetic Field Measurement in Prominences*

The pioneering studies summarized in Sect. 2.1 demonstrated the importance of the Hanle effect in measurement of prominence magnetic fields. Limitations of these early observations and their accompanying diagnostic techniques have been occulted in recent years as a result of the following advances.

Spectral Resolution and Sampling: House & Smartt (1982) reported the first systematic full-Stokes spectral profile measurements of He I D_3 multiplet in prominences. This spectral line contains several spectral components differing in sensitivity to the Hanle effect. When this added information is incorporated into the analysis it becomes possible to extract the full magnetic field vector. The earlier polarimetric measurements determined Stokes Q/I and U/I only, but as noted above and as pointed out by Landi Degl’Innocenti (1982), the Stokes V profile also provides information regarding the strength and orientation of the magnetic field. For stronger fields, the Stokes V profile will show the spectrally anti-symmetric signature arising from the Zeeman effect (splitting in wavelength of the Zeeman M -sublevels). The M -sublevels may also differ from their natural populations (atomic “orientation” and/or “alignment”) due to radiative effects, particularly from level crossings arising in the incomplete Paschen-Back effect (see Fig. 4 of Sahal-Brechot, Bommier, & Leroy 1977) and another “more subtle effect” mentioned by Landi Degl’Innocenti (1982).

Magnetic Field Measurements in the Infrared He I 10830Å line: Advancements in infrared detectors in recent times have permitted polarimetry of prominences in the He I infrared line at 10830Å. Like its counterpart He I D_3 , the 10830Å line is in fact a multiplet whose spectral components also differ in sensitivity to the Hanle effect.

Several instruments permit polarimetric measurements in He I 10830 Å, most notably the Tenerife Infrared Polarimeter (TIP, Collados *et al.* 2007). TIP observations of prominence magnetic fields have been reported by Trujillo Bueno *et al.* (2002), Merenda *et al.* (2006), Orozco Suárez, Asensio Ramos, & Trujillo Bueno (2013).

More Complete Quantum Mechanical Treatment of Polarization: Subtle effects, among them atomic orientation, give rise to observable signatures in all the polarization profiles, thereby providing unique new information regarding the magnetic field that would be unavailable from measurements of Stokes Q and U alone. The full treatment of the incomplete Paschen-Back effect and its influence on the populations of the Zeeman M -sublevels is a hallmark of many of the more recent studies (López Ariste & Casini 2002; López Ariste & Casini 2003; Casini *et al.* 2003; Merenda *et al.* 2006; Orozco Suárez, Asensio Ramos, & Trujillo Bueno 2013, Schmieder *et al.* 2013). Another effect is the possibility atomic polarization of the lower level of a transition influencing the observed polarization through selective absorption (Trujillo Bueno *et al.* 2002). The upper level of the weak blue component of He I 10830 Å line has total angular momentum quantum number $J = 0$, thus this line is intrinsically unpolarizable, so scattering polarization in this line must arise from *lower level polarization*. This polarization is observed in absorption in filaments seen against the solar disk, so the imbalance of the lower-level M -sublevels leads to this selective absorption of one polarization direction. Note that the lower term of He I D₃ is the upper term of He I 10830 Å. Being optically thin, the He I D₃ line will not show any polarization arising from a selective absorption process, but an imbalance in the lower level M -sublevels may, through statistical equilibrium, influence the upper levels. Through fitting observed profiles, Trujillo Bueno *et al.* (2002) provide an example of prominence polarization measurements in 10830 Å where the selective emission is influenced by lower level polarization. It is likely, then, that He I D₃ emission polarization will be influenced by polarization of its lower levels. It must be stressed that the complex physics involved in the scattering process leading to the Hanle effect needs to be treated in its full quantum mechanical generality, otherwise significant errors in the inference of magnetic fields will be encountered (Casini 2002).

Innovative Inversion Procedures: Quite a few assumptions needed to be invoked in order to produce Hanle effect diagrams for the optically-thick non-LTE, multi-dimensional H α line (Bommier *et al.* 1994). Furthermore, such diagrams fail to incorporate the polarization generated as a result of the Zeeman effect, even though it has been demonstrated that many prominences show Stokes V profiles that have the Zeeman-like anti-symmetry (Trujillo Bueno *et al.* 2002). Recent years have seen the development of inversion codes that incorporate most of the complex quantum electrodynamics effects shown to be important to the scattering of polarized light in prominences. Among these is the HAZEL code (Asensio Ramos, Trujillo Bueno, & Landi Degl'Innocenti 2008) that embraces both the Hanle and Zeeman effects for various geometries of arbitrary optical depth. The latter is especially important for the formation of the red blend of the He I 10830 Å line. The HAZEL code uses the standard Levenberg-Marquardt least squares minimization augmented with an algorithm to invoke a search of the entire parameter space in order to select the global minimum. The main drawback of this standard inversion scheme is that the procedure must do at least one forward computation of the radiative transfer for each iteration of the least-squares procedure, so the computations become very time-consuming. Another approach is the application of pattern recognition techniques to identify the best fit to observations of Stokes profiles derived from a physical model. López Ariste, Casini, and co-workers have successfully applied principal components analysis (PCA, see for example Rees *et al.* 2000) to invert prominence observations (López

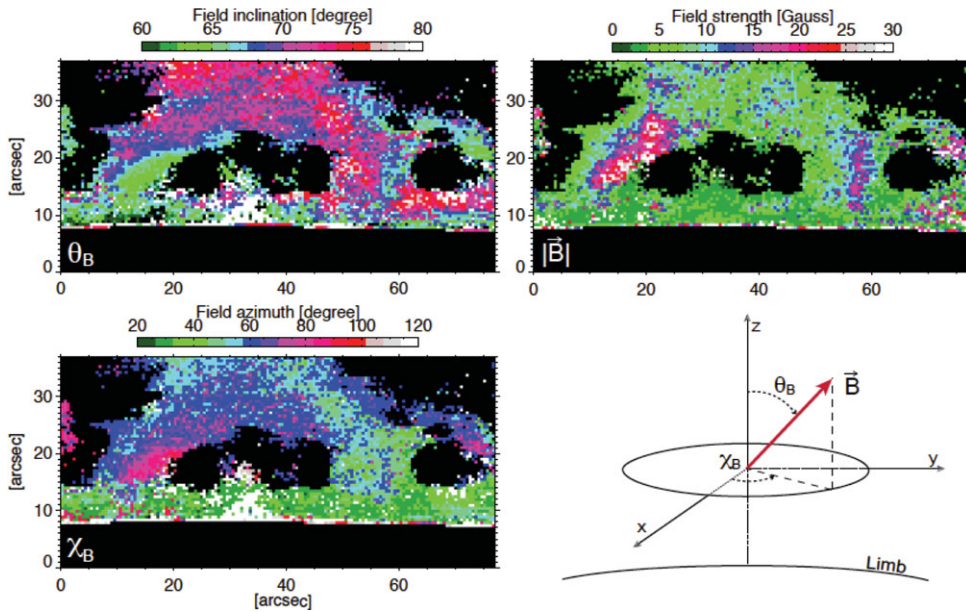


Figure 1. A two-dimensional map of the magnetic field vector within a prominence as inferred using the HAZEL procedure (see Sect. 2.2) is shown. This figure is adapted from Figure 3 of Orozco Suárez, Asensio Ramos, & Trujillo Bueno (2013). Shown as color images are the field strength and two angles defining the field orientation. Note that the field inclination to the local vertical θ_B is consistently large indicating fields close to horizontal. See online version of this article for color display.

Ariste & Casini 2002; Casini *et al.* 2003; Brown, López Ariste, & Casini 2003, Casini *et al.* 2009; Casini *et al.* 2013, Schmieder *et al.* 2013). A considerable initial investment in computation is needed at the outset to develop a suitably chosen database of synthetic Stokes profiles spanning physically realistic ranges of parameters describing the physical model, but once this “training data set” is in hand, the method allows a very rapid search for the model best fitting any observed set of Stokes profiles. Furthermore, PCA inversions *always* select the global best fit.

Measurements that Map the Solar Scene: Information on the spatial variation of the vector magnetic field within a prominence is of paramount importance to understanding the prominence phenomenon. Unlike vector field maps of the photosphere, authors often reported inference of a few scattered points within a prominence, or even more commonly measurements at only one spatial location. In order to acquire a S/N adequate for Hanle effect analysis, it was necessary to carry out observations with long integration times, thereby preventing measurements at high spatial and/or temporal resolution. Also, not until the modern era were spectro-polarimeters capable of two-dimensional maps. Casini *et al.* (2003) were among the first to report such a map. Figure 1 shows results from a recent application of the HAZEL code to prominence polarimetry in He I 10830 Å. The authors of that paper show that the strength of the field and its orientation do not vary rapidly from point-to-point, but there are significant variations of larger scale across the prominence. They also demonstrate that, like the earlier observational studies using the Hanle effect, the prominence fields are nearly horizontal. Recently, a similar result has been reached by Schmieder *et al.* (2013) from maps of the magnetic field of a prominence observed in He I D₃. Their analysis also reveals that the prominence fields are nearly horizontal with orientation varying little from parallel to the plane-of-the-sky.

Magnetic Field Measurements of Filaments Seen Against the Disk: The 10830 Å line has substantial optical depth in prominences, and for this reason it has been useful as a Hanle effect diagnostic of filaments seen against the solar disk. For quiescent filaments the Hanle effect provides an excellent diagnostic in He I 10830 Å because it affects the degree of line polarization for field strengths of a few Gauss. For stronger field strengths (in the saturation regime of the Hanle effect – between 10 - 100 Gauss for He I 10830 Å) the direction of linear polarization is an indicator of the orientation of the magnetic field in the plane of the sky, as is also the case for forbidden coronal emission lines. Of course, as the field strength increases, the Zeeman effect begins to produce measurable signatures in Stokes *V*. An early application of the Hanle effect to filaments on the disk was presented by Lin, Penn, & Kuhn (1998), but it was demonstrated subsequently that his approximate classical approach failed to account for important quantum effects (see the last paragraph of Casini *et al.* 2002). To date it appears that there have been no applications of the Hanle effect to infer the magnetic field in quiescent filaments, however recent studies of the magnetic structure of active region filaments, measured simultaneously in the chromosphere using He I 10830 Å and the photosphere using the nearby Si I line at 10827 Å have demonstrated the presence of rather strong fields (~ 600 Gauss) at both heights with a vertical shear of the field direction (Kuckein *et al.* 2009; Kuckein, Martínez Pillet, & Centeno 2012). Those authors concluded that the field strengths within the filament were strong enough that the polarization may be described by the Zeeman effect alone after obtaining similar results for the field using analysis that incorporates both the Zeeman effect and scattering polarization. Trujillo Bueno & Asensio Ramos (2007) find that polarization from the scattering process in He I 10830 Å in low-lying prominences and filaments may be significant for field strengths up to 1000 Gauss, however they reason that the anisotropy of the radiation field within the filament could be reduced considerably due to the optical thickness of the He I 10830 Å line, thereby drastically reducing the scattering polarization.

3. The Photospheric Magnetic Field Under Prominences

Observations of the photospheric magnetic field shed some light on evolution of prominences and their associated large-scale magnetic structures. Studies of the photospheric vector magnetic field under active region filaments (Lites 2005, Okamoto *et al.* 2009, Lites *et al.* 2010) reveal features of the photospheric vector magnetic field that evolve in a way that is consistent with the emergence of a flux rope into the atmosphere, rather than formation within the atmosphere itself. Figure 2, from Lites *et al.* (2010), documents one well-observed active region magnetic field below a filament. The orientation of the spatial fine structure in the transverse apparent flux density (left panel) coincides with the orientation of the inferred magnetic field vector (arrows in right panel), revealing the inverse configuration of the field at the photosphere. Of particular interest is the upper part of the filament channel that not only shows a pronounced inverse magnetic configuration, but also this segment of the filament is not bordered on either side by strong photospheric plage. This filament presents a clear imprint upon the photospheric magnetic field, but its magnetic buoyancy does not appear to be constrained from above by magnetic loops of the immediately surrounding fields. The mass of the filament itself may be the dominant counterbalance to its magnetic buoyancy – a circumstance that would be common in the buoyant rise of a massive flux rope from below the photosphere.

There are very few studies of the vector magnetic field in the photosphere below quiescent filaments because they have weak magnetic fields and often reside relatively high in

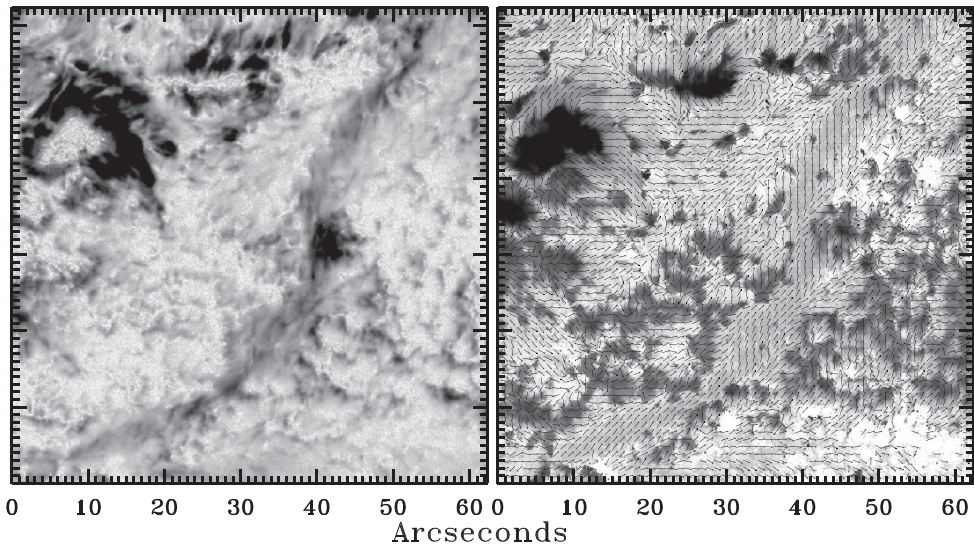


Figure 2. A filament channel whose evolution was documented by *Hinode*/SP observations reveals aspects suggesting that a flux rope emerged from below the photosphere. Left panel: the transverse apparent flux density is shown as a gray scale image with darker shades corresponding to higher values. The filament channel running from lower left to upper right is clearly distinguished by higher values of horizontal magnetic field strength. Right panel: intrinsic field strength is displayed as a gray scale with larger values corresponding to darker shades. The orientation of the horizontal component of the field is shown by arrows. The filament channel has rather uniform field strengths of ~ 500 Gauss. Many areas of the channel have inverse polarity suggesting a flux rope configuration. See Lites *et al.* (2010) for further details.

the corona. Furthermore, fields in the quiet photosphere that define the magnetic structure in the corona originate in the stronger photospheric flux tubes which, by nature, are strongly buoyant and therefore nearly vertical there. Hence, little can be learned about the topology of the field at much greater heights through measurement of the field vector at the photosphere. Nonetheless, López Ariste *et al.* (2006) did encounter a situation where an inverse magnetic configuration (a “bald patch”) was present under a filament “barbs”. Filament barbs are known to be extensions of cool prominence material downward toward the photosphere from the main body of the prominence. It is likely that the filament magnetic field has a flux rope topology that dips low enough at the barbs to impose its presence at the photospheric level.

4. Prospects for the Future

Our field is poised for rapid advancement of our understanding of prominence magnetic fields. Parallel developments in comprehensive understanding of the theory polarization via the scattering process in stellar atmospheres and advanced inversion methods based on pattern recognition techniques now provide us with tools for inference of magnetic fields in prominences, both above the limb and seen as filaments on the solar disk.

Spectro-polarimeters are now capable of routinely producing maps of active regions with full spectral and spatial coverage and techniques for observing in the near IR region open the possibility of detailed observations in He I 10830 Å. These developments notwithstanding, new observational facilities are needed totake full advantage of

advanced analysis techniques. At present, long integration times are required to achieve the S/N needed for quantitative analysis of the weak polarization signals from prominences. In practice, observations with current facilities require both spatial averaging and long integration times, with the result that the fine structure of prominences and filaments is essentially not observable when quantitative information on the polarization is required. This drawback may be addressed, of course, with larger aperture telescopes and more efficient polarimeters. We look to the future to the ATST and EST large solar telescopes to open the way to comprehensive, high-resolution observations from the ground. Another potentially dramatic advancement in observational capability would be the Japan/US/Europe *Solar-C* space mission that will be optimized for polarimetry of spectral features forming in the chromosphere. In the near future, we look to more modest advances from the ground-based Prominence Magnetometer (ProMag) instrument (<http://www.hao.ucar.edu/research/stsw/science/promag.php>) that will do spectro-polarimetry simultaneously in He I D₃, He I 10830 Å, and H α ; and the Japanese Chromospheric Lyman-Alpha SpectroPolarimeter (CLASP) rocket program (Kano *et al.* 2012) that will observe scattering polarization in Ly α .

Because filaments on the disk hold such great promise for understanding the detailed structure of prominence magnetic fields, observations of filament magnetic fields will become increasingly important. In order to interpret those disk observations it will be necessary for analysis tools to embrace the significant optical thickness of the spectral features that provide good magnetic field diagnostics (i.e., He I 10830 Å). Of course, CLASP observations will also require analyses that account for the significant optical depth in the Ly α line. The few studies of the evolution of the photospheric vector magnetic field under filaments suggest the emergence of a flux rope, but it is unclear if this is the usual situation for active region filaments. It is now possible to use the Solar Dynamics Observatory/HMI space instrument to obtain a continuous record of the vector magnetic field for *every* active region filament on the disk since early 2010. The results of such a study could be very revealing.

Acknowledgements

I thank the SOC of IAUS300 for the invitation to present this review, and R. Centeno for helpful suggestions on the manuscript. Work presented herein was supported in part under NASA contract NNM07AA01C for the *Hinode* program at LMSAL and HAO. The National Center for Atmospheric Research is sponsored by the National Science Foundation.

References

- Asensio Ramos, A., Trujillo Bueno, J., & Landi Degl'Innocenti, E. 2008, *ApJ*, 683, 542
- Bommier, V. 1980, *A&A*, 87, 109
- Bommier, V. & Leroy, J. L. 1998, in: Webb, D. F., Schmieder, B., & Rust, D. M. (eds.) *IAU Colloq. 167: New Perspectives on Solar Prominences*, (Astronomical Society of the Pacific Conference Series) 150, 434
- Bommier, V. & Sahal-Brechot, S. 1978, *A&A*, 69, 57
- Bommier, V., Sahal-Brechot, S., & Leroy, J. L. 1981, *A&A*, 100, 231
- Bommier, V., Sahal-Brechot, S., & Leroy, J. L. 1986, *A&A*, 156, 79
- Bommier, V., Landi Degl'Innocenti, E., Leroy, J.-L., & Sahal-Brechot, S. 1994, *Solar Phys.*, 154, 231
- Brown, A., López Ariste, A., & Casini, R. 2003, *Solar Phys.*, 215, 295
- Casini, R. 2002, *ApJ*, 568, 1056

- Casini, R., López Ariste, A., Tomczyk, S., & Lites, B. W. 2003, *ApJ*, 598, L67
- Casini, R., López Ariste, A., Paletou, F., & Léger, L. 2009, *ApJ*, 703, 114
- Casini, R., Asensio Ramos, A., Lites, B. W., & López Ariste, A. 2013, *ApJ*, 773, 180
- Collados, M., Lagg, A., Díaz Garcá A. J. J., Hernández Suárez, E., López López, R., Páez Mañá, E., & Solanki, S. K. 2007, in: Heinzl, P., Dorotovič, I., & Rutten, R. J. (eds.) *The Physics of Chromospheric Plasmas*, (Astronomical Society of the Pacific Conference Series) 368, 611
- Harvey, J. W. 1969, *Magnetic Fields Associated with Solar Active-Region Prominences* PhD thesis, (University of Colorado at Boulder)
- House, L. L. & Smartt, R. N. 1982, *Solar Phys.*, 80, 53
- Hyder, C. L. 1965, *ApJ*, 141, 1374
- Hyder, C. L. 1966, *ZfA*, 63, 78
- Kano, R. et al. 2012, in: *Society of Photo-Optical Instrumentation Engineers (SPIE) Conference Series*, (Society of Photo-Optical Instrumentation Engineers (SPIE) Conference Series) 8443
- Kuckein, C., Martínez Pillet, V., & Centeno, R. 2012, *A&A*, 539, A131
- Kuckein, C., Centeno, R., Martínez Pillet, V., Casini, R., Manso Sainz, R., & Shimizu, T. 2009, *A&A*, 501, 1113
- Landi Degl'Innocenti, E. 1982, *Solar Phys.*, 79, 291
- Landi Degl'Innocenti, E., Bommier, V., & Sahal-Brechot, S. 1987, *A&A*, 186, 335
- Leroy, J. L. 1977, *A&A*, 60, 79
- Leroy, J. L. 1978, *A&A*, 64, 247
- Leroy, J. L., Bommier, V., & Sahal-Brechot, S. 198, *Solar Phys.*, 83, 135
- Leroy, J. L., Bommier, V., & Sahal-Brechot, S. 1984, *A&A*, 131, 33
- Leroy, J. L., Ratier, G., & Bommier, V. 1977, *A&A*, 54, 811
- Lin, H., Penn, M. J., & Kuhn, J. R. 1998, *ApJ*, 493, 978
- Lin, Y., Wiik, J. E., Engvold, O., Rouppe van der Voort, L., & Frank, Z. A. (2005) *Solar Phys.*, 227, 283
- Lites, B. W. 2005, *ApJ*, 622, 1275
- Lites, B. W., Kubo, M., Berger, T., Frank, Z., Shine, R., Tarbell, T., Title, A., Okamoto, T. J., & Otsuji, K. 2010, *ApJ* 718, 474
- López Ariste, A., Casini, R., Paletou, F., Tomczyk, S., Lites, B. W., Semel, M., Landi Degl'Innocenti, E., Trujillo Bueno, J., & Balasubramaniam, K. S. 2005, *ApJ*. 621, L145
- López Ariste, A., Aulanier, G., Schmieder, B., & Sainz Dalda, A. 2006, *A&A*, 456, 725
- López Ariste, A. & Aulanier, G. 2007, in: Heinzl, P., Dorotovič, I., Rutten, R. J. (eds.) *The Physics of Chromospheric Plasmas*, (Astronomical Society of the Pacific Conference Series) 368, 291
- López Ariste, A. & Casini, R. 2002, *ApJ*, 575, 529
- López Ariste, A. & Casini, R. 2003, *ApJ*, 582, L51
- Mackay, D. H., Karpen, J. T., Ballester, J. L., Schmieder, B., & Aulanier, G. 2010, *Space Sci. Revs.*, 151, 333
- Okamoto, T. J., Tsuneta, S., Lites, B. W., Kubo, M., Yokoyama, T., Berger, T. E., Ichimoto, K., Katsukawa, Y., Nagata, S., Shibata, K., Shimizu, T., Shine, R. A., Suematsu, Y., Tarbell, T. D., & Title, A. M. 2009, *ApJ*, 697, 913
- Merenda, L., Trujillo Bueno, J., Landi Degl'Innocenti, E., & Collados, M. 2006, *ApJ*, 642, 554
- Orozco Suárez, D., Asensio Ramos, A., & Trujillo Bueno, J. 2013, in: *Highlights of Spanish Astrophysics VII*, 786
- Paletou, F. 2008, in: Charbonnel, C., Combes, F., & Samadi, R. (eds.) *SF2A-2008*, 559
- Paletou, F. & Aulanier, G. 2003, in: Trujillo-Bueno, J. & Sanchez Almeida, J. (eds.) *Solar Polarization*, (Astronomical Society of the Pacific Conference Series) 307, 458
- Rees, D. E., López Ariste, A., Thatcher, J., & Semel, M. 2000, *A&A*, 355, 759
- Rust, D. M. 1967, *ApJ*, 150, 313
- Sahal-Brechot, S., Bommier, V., & Leroy, J. L. 1977, *A&A*, 59, 223
- Schmieder, B., Gunár, S., Heinzl, P., & Anzer, U. 2007, *Solar Phys.*, 241, 53

- Schmieder, B., Kucera, T. A., Knizhnik, K., Luna, M., Lopez-Ariste, A., & Toot, D. 2013, *ApJ*, 777, 108
- Tandberg-Hanssen, E. 1970, *Solar Phys.*, 15, 359
- Trujillo Bueno, J. & Asensio Ramos, A. 2007, *ApJ*, 655, 642
- Trujillo Bueno, J., Landi Degl'Innocenti, E., Collados, M., Merenda, L., & Manso Sainz, R. 2002, *Nature*, 415, 403
- Zirin, H. & Severny, A. 1961, *The Observatory*, 81, 155